



Treatment of aqueous wastes contaminated with Congo Red dye by electrochemical oxidation and ozonation processes

Mohammed Faouzi Elahmadi^a, Nasr Bensalah^{b,*}, Abdellatif Gadri^{a,b}

^a School of Engineering of Gabes, Department of Chemical Engineering, 6072 Zrig, Gabes, Tunisia

^b Faculty of Sciences of Gabes, Department of Chemistry, 6072 Zrig, Gabes, Tunisia

ARTICLE INFO

Article history:

Received 8 January 2009

Received in revised form 26 February 2009

Accepted 26 February 2009

Available online 11 March 2009

Keywords:

Boron doped diamond anodes

Ozonation

Congo Red dye

Discoloration

Oxidation

Energy consumption

ABSTRACT

Synthetic aqueous wastes polluted with Congo Red (CR) have been treated by two advanced oxidation processes: electrochemical oxidation on boron doped diamond anodes (BDD-EO) and ozonation under alkaline conditions. For same concentrations, galvanostatic electrolyses have led to total COD and TOC removals but ozonation process can reach only 85% and 81% of COD and TOC removals, respectively. UV–vis qualitative analyses have shown different behaviors of CR molecules towards ozonation and electrochemical oxidation. Rapid discoloration has been observed during ozonation, whereas color persistence till the end of galvanostatic electrolyses has been seen during BDD-EO process. It seems that the oxidation mechanisms involved in the two processes are different: simultaneous destruction of azoic groups is suggested during ozonation process but consecutive destruction of these groups is proposed during BDD-EO. However, energetic study has evidenced that BDD-EO appears more efficient and more economic than ozonation in terms of TOC removals. These results have been explained by the fact that during BDD-EO, other strong oxidants electrogenerated from the electrolyte oxidation such as persulfates and direct-oxidation of CR and its byproducts on BDD anodes complement the hydroxyl radicals mediated oxidation to accomplish the total mineralization of organics.

© 2009 Elsevier B.V. All rights reserved.

1. Introduction

Recently, wastewater treatment and water reuse have taken much more interest. Biological treatments which are simple and most economic methods have been largely used to treat wastewaters, but in many cases these methods have been inefficient to degrade toxic and resistant organic pollutants. Azo dyes are of high toxicity and even carcinogenic to the animals and human and they are not readily degradable [1]. Wastewaters containing such type of dyes are known to be highly resistant to the traditional physical, chemical and biological methods [1–5]. Different technologies have been tested for dye removal including adsorption [6], coagulation, flocculation [7] and reverse osmosis processes [8,9]. Although these methods resulted in a significant color removal, they were costly to apply in the actual field, enable to meet the discharge criteria of wastewater in terms of chemical oxygen demand and they all end up in producing a secondary waste product which needs to be tackled further. Advanced oxidation processes (AOPs) could be alternative methods able to achieve total mineralization of organic pollutants through the production of powerful oxidizing agent as hydroxyl radicals (HO[•]). AOPs have been employed

to treat dye-contaminated wastewater effluents and in many cases the macromolecule is completely broken down to water and carbon dioxide [10–12].

In this context, electrochemical oxidation on boron doped diamond (BDD) anodes (BDD-EO) and ozonation at alkaline medium could be considered as suitable AOPs for treatment of wastewaters containing organic pollutants. Two technologies have been widely studied for the treatment of wastewaters containing great variety of organics. The most important results of these studies are that these technologies let achieving high chemical oxygen demand (COD) and total organic carbon (TOC) removals [14–30]. BDD-EO and ozonation present several common points in their procedures. The main common points are: (i) both technologies supply, *in situ*, HO[•] radicals in large amounts as necessary as incineration of organic matter could be done [31–35], (ii) the processes require electrical energy supply to be carried on and to produce strong oxidants, and (iii) they do not produce secondary pollution.

The goal of this work is to compare the two advanced oxidation processes: BDD-EO and ozonation (at pH 12) in the treatment of dyeing wastewaters. Congo Red (CR), being a typical azoic dye presenting two azo bonds (–N=N–) chromophores in its molecular structure, was selected as a model dyeing pollutant. The dye was selected due to its complex chemical structure (Fig. 1), high molecular weight, high solubility in water and its persistence one it is discharged into natural environment [36–38]. The degradation

* Corresponding author. Tel.: +216 75392600; fax: +216 75392421.

E-mail address: nasr.bensalah@issatgb.rnu.tn (N. Bensalah).

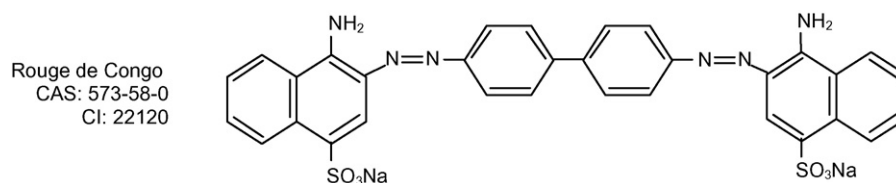


Fig. 1. Chemical structure of Congo Red.

and mineralization of CR by both techniques were followed by COD, TOC, UV–vis analyses. The results obtained will be used to investigate the degradation pathways involved in these processes and enhance our understanding about role of hydroxyl radicals in the two advanced oxidation processes.

2. Experimental details

2.1. Chemicals

CR was of analytical grade and purchased from Fluka. The other chemicals were of analytical grade and purchased from Sigma–Aldrich or Merck and used as-received. All solutions were prepared with deionized water having $18 \text{ m}\Omega \text{ cm}^{-1}$ resistivity from a Mill-Q™ system.

2.2. Analytical procedure

The carbon concentration was monitored using a Shimadzu TOC-5050 analyzer. Chemical oxygen demand (COD) was determined using a HACH DR2000 analyzer. UV–vis spectra were obtained using a Shimadzu 1603 spectrophotometer and quartz cells. To eliminate the influence of pH on the evolution of UV–vis spectra, all solutions were buffered at pH 7 by phosphate buffer solution just before drawing the spectra.

2.3. Determination of the oxygen-equivalent chemical-oxidation capacity (OCC)

To quantify the amount of oxidant supplied in the oxidation process, the oxygen-equivalent chemical-oxidation capacity (OCC) parameter is determined for each AOP technique used in this work. OCC is defined as the kg of O_2 that are equivalent to the quantity of oxidant reagents used in each AOP to treat 1 m^3 of wastewater [16,18]. Taking into account Faraday number in the case of EO and the number of electrons exchanged in the ozone reduction, the following equations are obtained:

$$1 \text{ OCC (kg O}_2 \text{ m}^{-3}) = 0.298Q \text{ (kA h m}^{-3}) \quad (1)$$

$$1 \text{ OCC (kg O}_2 \text{ m}^{-3}) = 1.000[\text{O}_3] \text{ (kg O}_3 \text{ m}^{-3}) \quad (2)$$

2.4. Conductive-diamond electrochemical oxidation

In this work, the BDD-EO assays were carried out in a single compartment electrochemical flow-cell as it is described by previous works [16,18]. Diamond-based material was used as anode and stainless steel (AISI 304) as cathode. Both electrodes were circular (10 cm diameter) with a geometric area of 78 cm^2 and an electrode gap of 0.9 cm. The wastewater was stored in a glass tank (0.6 L) and circulated through the electrolytic cell by means of a centrifugal pump (flow rate 2.5 L min^{-1}). A thermostatic bath was used to maintain the temperature at the desired set point. The experimental setup also contained a cyclone for gas–liquid separation, and a gas absorber to collect the carbon dioxide contained in the gases evolved from the reactor into sodium hydroxide. Boron doped diamond films were provided by CSEM (Switzerland) and synthesized

by the hot filament chemical vapour deposition technique (HF CVD) on single-crystal p-type Si (1 0 0) wafers (0.1 cm, Siltronix). Electrolyses were carried out in galvanostatic mode. During the electrolyses no control of pH was carried out.

2.5. Ozonation

Ozonation experiments were carried out by continuously feeding an ozone–oxygen gas stream in a mixed semi-batch bubble reactor (continuous for gas and batch for liquid). This reactor consists of a 2.5 L jacketed cylindrical Pyrex glass tank equipped with a porous gas distribution plate and baffles to increase the capacity of absorption of ozone. A mechanical stirrer and a recycle pump (Emapompe, model P 022 Plastomec) are also used to promote the absorption of ozone and to obtain good mixing conditions. Pure oxygen taken from a commercial cylinder was fed into an ozone generator (Ambizon, Model GMF-10, Sistemas y Equipos de Ozonización S.L., Madrid, Spain) which is able to produce a maximum mass flow rate of 10 g h^{-1} . In the generator outlet, the stream was dried with a sample conditioner (Sample conditioning system, model SC-010-R AFX, Sistemas y Equipos de Ozonización S.L., Madrid, Spain). The concentration of ozone in the gas at the reactor outlet and inlet was measured with an ozone meter (Ozone analyser, Model H1 AFX, Sistemas y Equipos de Ozonización S.L., Madrid, Spain) and its calibration was carried out iodometrically [39]. Dissolved ozone concentration in the liquid phase was determined spectrophotometrically (600 nm) from discoloration of the resulting solution, by the Karman indigo method [40]. In the experiments described in this work, the ozone–oxygen mixture gas stream was sparged with a constant flow rate of 0.5 L min^{-1} (flow controller Cole Parmer, model #: 32907-39) and the average production of ozone was around 1 g h^{-1} . The volume of wastewater treated in each assay was 2 L and it was placed inside the reactor prior to the experiments. To increase the mixing conditions, the stirring rate of the mechanical stirrer was adjusted to 550 rpm and the flow recycled to 67.5 L h^{-1} . The ozone generator was switched on prior to the experiments, and only when the desired ozone percentage in the ozone–oxygen gas was reached (steady state conditions) the ozone–oxygen mixture gas stream started to be sparged into the reactor. During the experiments sodium hydroxide was added to the reactor to maintain the pH in a set point close to 12 ± 0.1 . According to literature [41,42], this is an optimum pH to promote the generation of hydroxyl radicals due to the radical decomposition of the ozone molecules. The temperature was also maintained during operation at 25°C using a thermostatic bath by circulating the water through the jacket reactor.

3. Results and discussion

3.1. Electrochemical oxidation process

Galvanostatic electrolyses of aqueous solutions containing CR were carried out under a current density of 30 mA cm^{-2} and at a temperature of 25°C and in presence of $5 \text{ g L}^{-1} \text{ Na}_2\text{SO}_4$. These operating conditions have been chosen considering that in previous works [13–23]; it has been shown that in sulfate medium

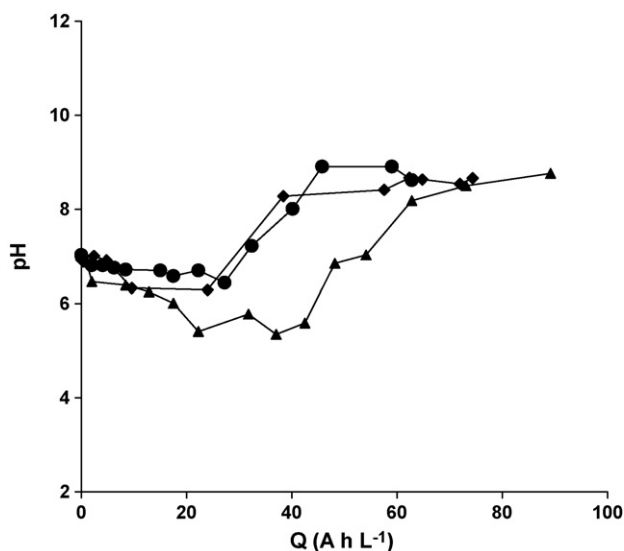


Fig. 2. pH evolution versus specific electric charge passed during electrolyses of (●) 0.1 g L⁻¹, (▲) 0.5 g L⁻¹ and (◆) 1.0 g L⁻¹ CR-polluted aqueous solutions. Operating conditions: anode: BDD ($S=78\text{ cm}^2$); cathode: stainless steel ($S=78\text{ cm}^2$); current density: $j=30\text{ mA cm}^{-2}$; $T=25\text{ }^\circ\text{C}$; electrolyte: $5\text{ g L}^{-1}\text{ Na}_2\text{SO}_4$; $\text{pH}_0=7$.

more strong oxidants could be electrogenerated from the oxidation of electrolyte at BDD surface which can mediate the oxidation of organics, but the use of high current densities decreases the electrochemical treatment efficiency and the increase of temperature has no significant influence on the overall kinetics of the process. The electrolyses were followed by measurements of pH, COD, TOC and UV-vis spectra.

Fig. 2 presents the evolution with specific electric charge of pH during galvanostatic electrolyses ($j=30\text{ mA cm}^{-2}$) on BDD anodes of aqueous solutions ($5\text{ g L}^{-1}\text{ Na}_2\text{SO}_4$) polluted with CR at different concentrations. As it can be seen, the pH has a little decrease before being stabilized at pH 9 for all initial concentrations but the decrease of pH is more significant for high concentrated solutions. To explain the pH evolution it should be taken into account that the pH of medium depends largely on cathodic and anodic processes and intermediates acid–base properties.

At the cathode, water reduction provides hydroxyl ion as it is given by Eq. (3):



At the anode, reactions below can be suggested to be happened:



R refers to CR or intermediates and P refers to byproducts. In this way, pH variation depends largely on electrode process predominance. Deprotonation (Eqs. (4) and (5)) decreases the pH value and oppositely hydroxide ion formation (Eq. (3)) increases this value. It seems that the proton generation rate on the anode is lower than that of hydroxyl anions at the cathode. Thus, the small amounts of protons generated at the anode partially compensate the anions generated at the cathode and, consequently, the pH increases. Moreover, at the beginning of the process there are more protons generated by reaction (4) and then a decrease of pH can be observed especially when high concentrations of CR solutions are electrolyzed. Furthermore, the cleavage of azoic groups can lead to aniline derivatives formation (alkaline character) which can explain also the pH increase. It should be noted that similar results have

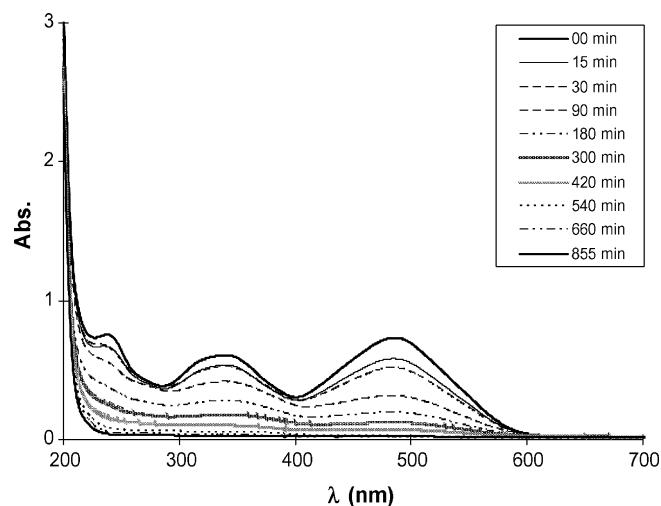


Fig. 3. Evolution of UV-vis spectra during BDD-EO of aqueous solution polluted with 0.5 g L^{-1} of CR. Operating conditions: anode: BDD ($S=78\text{ cm}^2$); cathode: stainless steel ($S=78\text{ cm}^2$); current density: $j=30\text{ mA cm}^{-2}$; $T=25\text{ }^\circ\text{C}$; electrolyte: $5\text{ g L}^{-1}\text{ Na}_2\text{SO}_4$; $\text{pH}_0=7$.

been reported by several authors in the study of BDD-EO of other dyes [16,17].

Fig. 3 presents evolution with time of UV-vis spectra during galvanostatic electrolysis of aqueous solution ($5\text{ g L}^{-1}\text{ Na}_2\text{SO}_4$) contaminated with 0.5 g L^{-1} CR. Three absorbance bands are observed at 237, 334 and 482 nm. Bands situated in UV region of spectra can be attributed to $\pi \rightarrow \pi^*$ transition in aromatic rings but the band of visible region can be due to azoic group transition. As it can be seen, continuous and simultaneous decrease of the band intensities was observed from the beginning of electrolysis. These bands disappeared after 540 min electrolysis. Total disappearance of the three bands suggests that no more aromatic intermediates exist in the water. These results show that total degradation of CR and its aromatic intermediates has been achieved by BDD-EO.

It seems that complex oxidation mechanism takes place during BDD-EO of CR aqueous solution. The fact is related to the persistence of visible band till the end of experiment and non-increase in intensities of UV bands and/or non-appearance of new UV bands. These results can be explained by the two following ideas:

- CR still is the main compound in the solution during galvanostatic electrolyses (persistence of visible band) and its aromatic intermediates generated during BDD-EO starts their degradation once they are formed (non-increase in intensities of UV bands and/or non-appearance of new UV bands).
- Consecutive destruction mechanism of azoic groups is involved (persistence of visible band) and the degradation byproducts absorb at same wavelengths than mother compound (non-increase in intensities of UV bands and/or non-appearance of new UV bands).

Fig. 4 presents the influence of CR concentration on the evolution with specific electric charge of COD and TOC during galvanostatic electrolyses ($j=30\text{ mA cm}^{-2}$) BDD anodes of aqueous solutions ($5\text{ g L}^{-1}\text{ Na}_2\text{SO}_4$) containing CR at different concentrations. High COD and TOC removals have been obtained by BDD-EO in regardless of CR concentration. Electrolyses of low organic matter concentrated solutions lead to total COD and TOC removals but the electrolyses of high loaded solutions can reach only 85% of COD removal and 81% of TOC removal. This result maybe explained by the accumulation of aliphatic carboxylic acids at the end of the treatment when high CR concentrations were electrolyzed. The

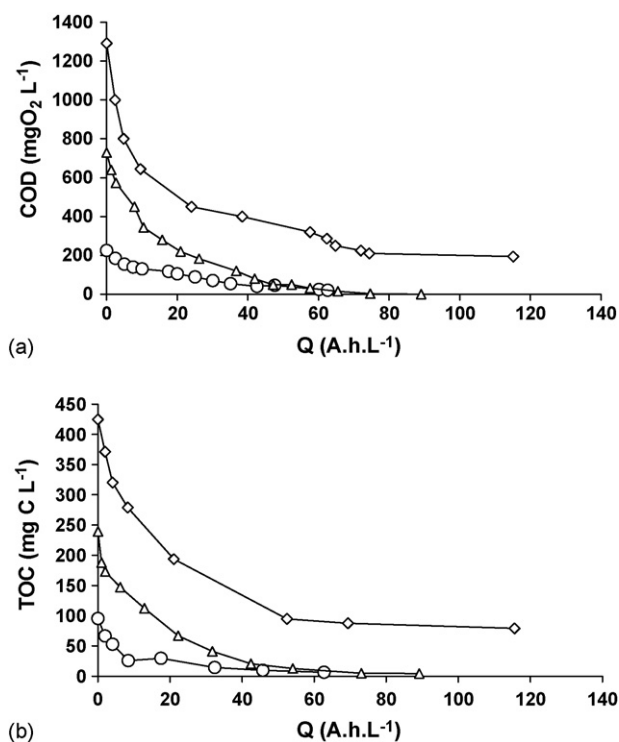


Fig. 4. Changes in the COD (a) and in the TOC (b) with the specific electric charge passed during electrolyses of (○) 0.1 g L⁻¹, (△) 0.5 g L⁻¹ and (◇) 1.0 g L⁻¹ CR-polluted synthetic wastes. Operating conditions: anode: BDD ($S=78\text{ cm}^2$); cathode: stainless steel ($S=78\text{ cm}^2$); current density: $j=30\text{ mA cm}^{-2}$; $T=25\text{ }^\circ\text{C}$; electrolyte: $5\text{ g L}^{-1}\text{ Na}_2\text{SO}_4$; $\text{pH}_0\ 7$.

continuous decrease of TOC shows that organic matter mineralization takes place from the beginning of electrolyses and that CO₂ is the sole final product of BDD-EO of this azoic dye. It is remarkable that the specific electrical charge required to achieve same COD and TOC removals is not proportional to CR concentration and the curves COD = $f(Q)$ have an exponential shape. These results indicate that the electrochemical process is mass transfer controlled as it was widely mentioned in literature [13–23].

3.2. Ozonation process

Ozonation is one of the most widely used advanced oxidation technologies for wastewater treatment. Ozone is itself a very powerful oxidant ($E^0 = 2.07\text{ V/SHE}$) and, in certain conditions, it can be decomposed and lead to the formation of hydroxyl radicals (i.e. at pH close to 12, which is going to be the conditions used in this work). In this later case, the process efficiencies are strongly increased [34].

Fig. 5 shows changes with time in the UV–vis spectra during the ozone treatment of synthetic wastes polluted with 0.5 g L^{-1} CR. The initial UV–vis spectrum of this compound is characterized by the presence of three bands at 237, 334 and 482 nm, which is similar to that observed during CR bulk electrolyses. As it can be observed, the intensities of these bands decrease continuously and disappear at the same time, after 60 min ozonation. The disappearance of the visible band is accompanied by total discoloration of the solution. Total discoloration of the solution results from the destruction of two azoic bonds present in CR chemical structure. As it can be seen also, an appearance of a new band situated at 215 nm was observed from the early minutes of ozonation experiment. This band increases in intensity when the intensities of other bands are decreasing, after the total disappearance of the bands observed in the initial solution, its intensity decreases slowly but it cannot be totally disappeared and persist till the end of exper-

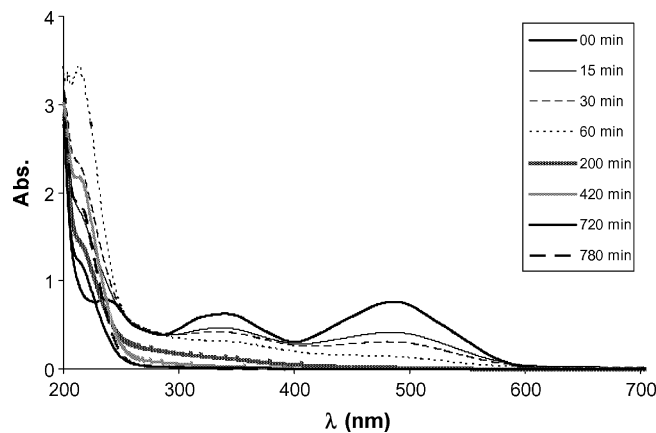


Fig. 5. Evolution of UV–vis spectra during ozonation of aqueous solution polluted with 0.5 g L^{-1} CR. Operating conditions: ozone production: 1 g h^{-1} ; $V=2\text{ L}$; $\text{pH}\ 12$; $T=25\text{ }^\circ\text{C}$.

iment. These results show that ozonation lead to rapid and total discoloration of CR aqueous solution. Moreover, it appears that simultaneous destruction mechanism of azoic groups is involved during ozonation of CR solutions.

These results seem to be different from those obtained during galvanostatic electrolyses on BDD anode of the same CR solution. Fig. 6 illustrates the evolution of visible band absorbance removal during BDD-EO and ozonation of 0.5 g L^{-1} CR aqueous solutions. This figure shows that total disappearance of visible band during ozonation is much more rapid than that during BDD-EO. This means that the destruction of azo groups is more rapid in ozonation than in BDD-EO. This observation can be related to the mechanism involved in each process. Selective chemical reaction of molecular ozone with azoic group ($-\text{N}=\text{N}-$) looks to be the main reaction at the beginning of ozonation process which leads to simultaneous breaking of azoic bonds and accelerates the discoloration of CR aqueous solution. Neither direct electron transfers at BDD anode, nor mediated oxidation by hydroxyl radicals (non-selective oxidation), can be able to destruct simultaneously the azoic two bonds and consecutive dissociation mechanism is involved during BDD-EO of CR aqueous solution which delay the discoloration of the solution to the end of electrochemical treatment. However, only BDD-EO leads to total disappearance of all the UV–vis absorbance bands indicating

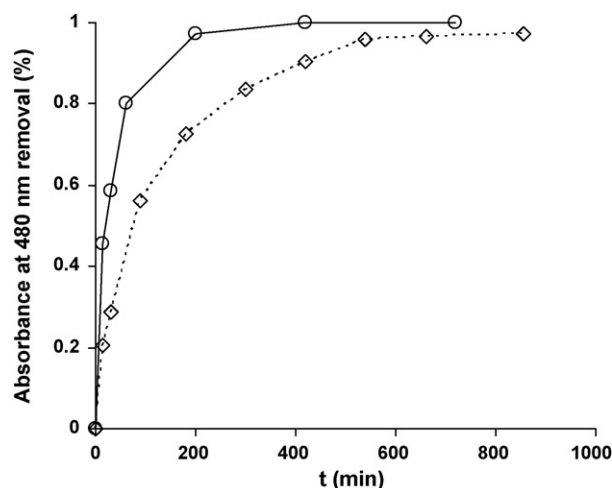


Fig. 6. Abatement of absorbance at 480 nm during the treatment of 0.5 g L^{-1} aqueous solution by (○) BDD-EO and (◇) ozonation. Operating conditions: BDD-EO—anode: BDD ($S=78\text{ cm}^2$); cathode: stainless steel ($S=78\text{ cm}^2$); $j=30\text{ mA cm}^{-2}$; $T=25\text{ }^\circ\text{C}$; $5\text{ g L}^{-1}\text{ Na}_2\text{SO}_4$; $\text{pH}_0\ 7$; ozonation—ozone production: 1 g h^{-1} , $V=2\text{ L}$, $\text{pH}\ 12$, $T=25\text{ }^\circ\text{C}$.

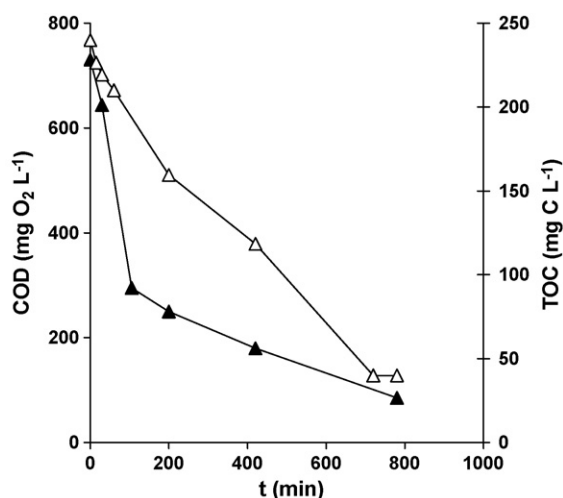


Fig. 7. Changes in the COD (▲) and in the TOC (△) during ozonation of 0.5 g L⁻¹ CR-polluted aqueous solution. Operating conditions: ozone production: 1 g h⁻¹, V=2 L, pH 12, and T=25 °C.

that total transformation of organic matter into CO₂ and aliphatic carboxylic acids. The later result cannot be reached by ozonation process which is inefficient in the final steps of degradation of some aromatic intermediates.

Fig. 7 shows the evolution of chemical oxygen demand (COD) and total organic carbon (TOC) during ozonation of synthetic wastewaters polluted with 0.5 g L⁻¹ RC at pH 12. As it can be observed, both parameters (COD and TOC) are satisfactorily reduced during the treatment by ozonation of 0.5 g L⁻¹ CR aqueous solution. Changes in the TOC indicate that carbon dioxide is formed from the very early oxidation stages. At the beginning of process, the COD decrease is more abrupt than TOC which indicates that the first step of ozonation leads to the formation of many intermediates with low CO₂ production rate. This suggests that treatment with ozone of a solution polluted with CR begins by the fragmentation of the initial structure to aromatic compounds then to aliphatic compounds. As it can be observed, the ozonation process can be used to treat this kind of actual wastewater. However, it is not able to achieve the complete mineralization of organics and a significant concentration of organic carbon (around 40 mg CL⁻¹) remains at the end of the process.

These results are different from those obtained with BDD-EO. The different behaviors observed for the two oxidation technologies studied here, have to be explained in terms of the oxidation mechanisms involved in each process. It is supposed that in these processes, the hydroxyl radicals are implicated in the oxidation [13–23], but according to the results, these differences have to be explained by the action of other oxidants. In the case of BDD-EO, the higher efficiencies help to confirm that there are other important oxidation processes that complement the hydroxyl radicals mediated oxidation [14–17]. Among them, two can be of special importance: the direct electro-oxidation on the BDD surface and the oxidation mediated by other electrochemically formed compounds generated in this electrode, due to the oxidation of sulfates such as peroxomonosulfates and peroxodisulfates [43]. In the same way, the good results observed at the beginning of ozonation process can be explained by the effect of the molecular ozone, which is selective oxidant for breaking (–N=N–) bonds but less powerful than hydroxyl radicals [44]. The low oxidation power of the molecular ozone explains the detection of refractory carbon at the end of ozonation treatment, in which the action of the hydroxyl radicals is, probably, the lone oxidative mechanism.

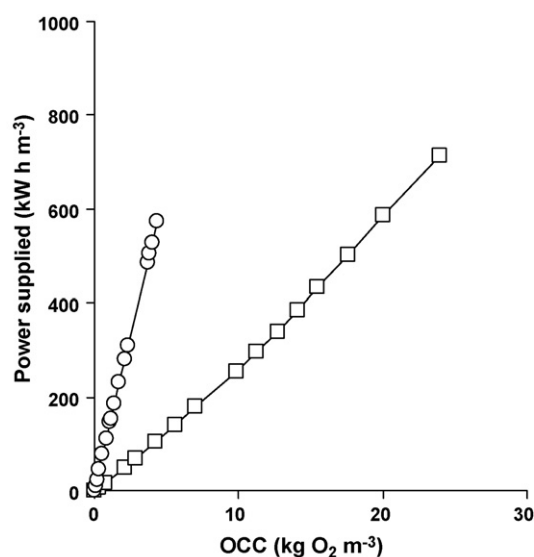


Fig. 8. Evolution of the supplied power versus OCC during the treatment of 0.5 g L⁻¹ aqueous solution by BDD-EO (□) and ozonation (○) processes. Operating conditions: BDD-EO—anode: BDD (S=78 cm²); cathode: stainless steel (S=78 cm²); j=30 mA cm⁻²; T=25 °C; 5 g L⁻¹ Na₂SO₄; pH₀ 7; ozonation—ozone production: 1 g h⁻¹, V=2 L, pH 12, T=25 °C.

3.3. Energy requirements

The comparison of the results obtained by BDD-EO and ozonation can be used to estimate energy requirement and economic conditions in these processes. To compare the results obtained with different oxidation technologies in terms of equivalent doses of oxidants, a new parameter has been recently proposed in literature: the OCC [16,18]. This parameter informs about the chemical efficiency of the oxidants used in each process and it quantifies the oxidants added to the waste with the same arbitrary units (kg O₂ m⁻³ of wastewater).

Fig. 8 presents evolution of the supplied power versus oxygen-equivalent chemical-oxidation capacity provided to oxidation media during BDD-EO (j=30 mA cm⁻²) and ozonation (1 g O₃ h⁻¹) treatments. As it can be seen, the supplied power increases linearly with OCC for the two processes. For the same OCC value, the energy required for ozonation is much higher than that required for BDD-EO which indicates that BDD-EO is more efficient than ozonation. On the other hand, Fig. 9 shows the evolution with OCC of TOC removal during BDD-EO (j=30 mA cm⁻²) and ozonation (1 g O₃ h⁻¹) of 500 ppm CR aqueous solutions. As it can be observed, for low OCC values, efficiencies of both BDD-EO and ozonation are similar. However, ozonation is not able to achieve percentage of TOC elimination higher than 85%, whereas BDD-EO allows attaining the almost complete mineralization. Fig. 10 shows evolution of power consumption with TOC removal during the treatment of 0.5 g L⁻¹ CR aqueous solutions by BDD-EO and ozonation. As it can be observed, energy requirements increase linearly up to 80% of TOC removal for the two processes but the energy consumption during ozonation increases more rapidly than that during BDD-EO process. For example to reach 80% of TOC removal, 528 kWh m⁻³ is required by ozonation but only 254 kWh m⁻³ is consumed during BDD-EO indicating that BDD-EO is more economic than ozonation. However, it is clear that the energy consumption versus TOC removal during BDD-EO becomes much more important to achieve total mineralization. The differences observed in both oxidation technologies are indicative of the generation of high concentration of intermediates (mainly carboxylic acid) that are accumulated in the system during ozonation. The lower oxidizability of the carboxylic

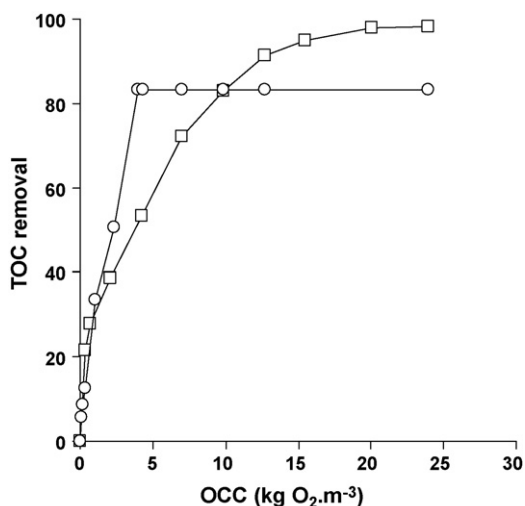


Fig. 9. Evolution of TOC removal versus OCC during the treatment of 0.5 g L⁻¹ aqueous solution by BDD-EO (□) and ozonation (○) processes. Operating conditions: BDD-EO—anode: BDD ($S=78\text{ cm}^2$); cathode: stainless steel ($S=78\text{ cm}^2$); $j=30\text{ mA cm}^{-2}$; $T=25\text{ }^\circ\text{C}$; 5 g L⁻¹ Na₂SO₄; pH₀ 7; ozonation—ozone production: 1 g h⁻¹, $V=2\text{ L}$, pH 12, $T=25\text{ }^\circ\text{C}$.

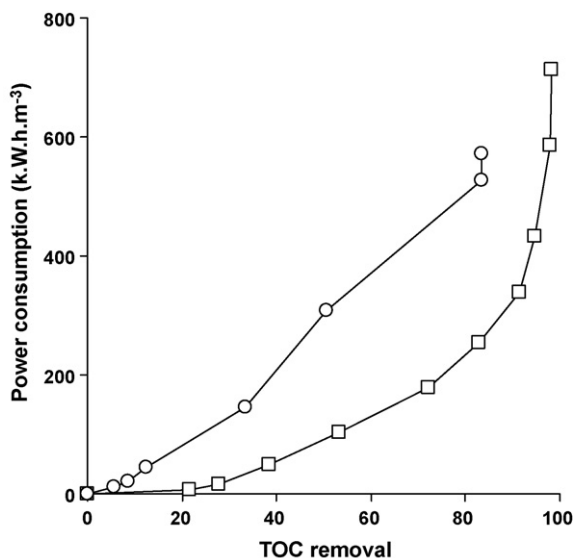


Fig. 10. Evolution of power consumption versus TOC removal during the treatment of 0.5 g L⁻¹ aqueous solution by BDD-EO (□) and ozonation (○) processes. Operating conditions: BDD-EO—anode: BDD ($S=78\text{ cm}^2$); cathode: stainless steel ($S=78\text{ cm}^2$); $j=30\text{ mA cm}^{-2}$, $T=25\text{ }^\circ\text{C}$, 5 g L⁻¹ Na₂SO₄, pH₀ 7; ozonation—ozone production: 1 g h⁻¹, $V=2\text{ L}$, pH 12, $T=25\text{ }^\circ\text{C}$.

acids towards ozonation can be explained by the feebler activity of molecular ozone and hydroxyl radicals over these intermediates. The high efficiency of BDD-EO is related to the existence of other important oxidation mechanisms such as persulfate oxidation and direct-oxidation of CR and byproducts on BDD anodes. Changes in energy requirements during BDD-EO can be explained by mass transfer limitations in the final steps of electrochemical process.

4. Conclusion

The main conclusions deduced from this work can be summarized in these points:

- Both BDD-EO and ozonation can be successfully used to treat aqueous solutions containing Congo Red azoic dye. BDD-EO can

achieve the almost total COD and TOC removals but ozonation at alkaline medium can reach only 85% and 81% of COD and TOC removals, respectively.

- During BDD-EO the persistence of visible band till the end of experiment and non-increase in intensities of UV bands and/or non-appearance of new UV bands are indicative of consecutive destruction mechanism of azoic groups and formation of degradation byproducts which absorb at same wavelengths than mother compound.
- The influence of CR initial concentration shows that specific electrical charge required to achieve same COD and TOC removals is not proportional to CR concentration and that exponential profile of COD versus specific electrical charge is observed in all cases in the range of concentration studied here. These results point to mass transfer control of the overall kinetics.
- The evolution of UV-vis spectra during ozonation process lead to more rapid discoloration of CR aqueous solution and appearance of new UV band which is indicative of simultaneous destruction of azo groups and formation of different aromatic intermediates.
- The energy requirements evolution with OCC and TOC removal during BDD-EO and ozonation show that BDD-EO is more efficient and more economic than ozonation in the treatment of this kind of wastewaters.
- The differences observed between the two oxidation technologies studied here, have to be explained in terms of the oxidation mechanisms involved in each process. The simultaneous destruction mechanism suggested for ozonation can be explained by the effect of the molecular ozone, which is selective oxidant for breaking ($-N=N-$) bonds. The high efficiency of BDD-EO is related to the complement hydroxyl radicals mediated oxidation with other important oxidation mechanisms such as indirect persulfate oxidation and direct-oxidation of CR and byproducts on BDD anodes.

Acknowledgements

The authors would like to acknowledge Prof. Manuel A. Rodrigo (University of Castilla-La-Mancha, Spain) for his gracious assistance. Dr. Nasr Bensalah thankfully acknowledges Prof. William J. Cooper (University of California, Irvine, USA) and US Department of State for financial support through Fulbright scholar program.

References

- [1] E. Forgacs, T. Cserhati, G. Oros, Removal of synthetic dyes from wastewaters: a review, *Environ. Int.* 30 (2004) 953–971.
- [2] I.M. Banat, P. Nigam, D. Singh, R. Marchant, Microbial decolorization of textile dye-containing effluents: a review, *Bioresour. Technol.* 58 (1996) 217–227.
- [3] P.C. Vandavivre, R. Biznchi, W. Vesstrae, Treatment and reuse of wastewater from the textile wet-processing industry: review of emerging technologies, *J. Chem. Technol. Biotechnol.* 72 (1998) 289–302.
- [4] E. Razo-Flores, M. Luijten, B. Donlon, G. Lettinga, J. Field, Biodegradation of selected azo dyes under methanogenic conditions, *Water Sci. Technol.* 36 (1997) 65–72.
- [5] D. Georgiou, C. Metallinou, A. Aivasidis, E. Voudrias, K. Gimouhopoulos, Decolorization of azo-reactive dyes and cotton-textile wastewater using anaerobic digestion and acetate-consuming bacteria, *Biochem. Eng. J.* 19 (2004) 75–79.
- [6] M. Xu Zhu, L. Lee, H.H. Wang, Z. Wang, Removal of an anionic dye by adsorption/precipitation processes using alkaline white mud, *J. Hazard. Mater.* 149 (2007) 735–741.
- [7] V. Golob, A. Vinder, M. Simonič, Efficiency of the coagulation/flocculation method for the treatment of dyebath effluents, *Dyes Pigments* 67 (2005) 93–97.
- [8] N. Al-Bastaki, Removal of methyl orange dye and Na₂SO₄ salt from synthetic waste water using reverse osmosis, *Chem. Eng. Process.* 43 (2004) 1561–1567.
- [9] C. Suksaroj, M. He' ran, C. Allègre, F. Persin, Treatment of textile plant effluent by nanofiltration and/or reverse osmosis for water reuse, *Desalination* 178 (2005) 333–341.
- [10] H. Lachheb, E. Puzenat, A. Houas, M. Ksibi, E. Elaloui, Ch. Guillard, J.-M. Herrmann, Photocatalytic degradation of various types of dyes (Alizarin S, Crocein Orange G, Methyl Red, Congo Red, Methylene Blue) in water by UV-irradiated titania, *Appl. Catal. B: Environ.* 39 (2002) 75–90.
- [11] I. Arslan-Alaton, I.A. Bacioglu, D.W. Bahnemann, Advanced oxidation of a reactive dyebath effluent: comparison of O₃, H₂O₂/UV-C and TiO₂/UV-A processes, *Water Res.* 36 (2002) 1143–1154.

- [12] H.-Y. Shu, C.-R. Huang, Degradation of commercial azo dyes in water using ozonation and UV enhanced ozonation process, *Chemosphere* 31 (1995) 3813–3825.
- [13] G. Chen, Electrochemical technologies in wastewater treatment, *Sep. Purif. Technol.* 38 (2004) 11–13.
- [14] C.A. Martínez-Huitle, S. Ferro, Electrochemical oxidation of organic pollutants for the wastewater treatment: direct and indirect processes, *Chem. Soc. Rev.* 35 (2006) 1324–1340.
- [15] B. Louhichi, M.F. Ahmadi, N. Bensalah, A. Gadri, M.A. Rodrigo, Electrochemical degradation of an anionic surfactant on boron-doped diamond anodes, *J. Hazard. Mater.* 158 (2008) 430–437.
- [16] P. Cañizares, A. Gadri, J. Lobato, N. Bensalah, R. Paz, M.A. Rodrigo, C. Saez, Electrochemical oxidation of azoic dyes with conductive-diamond anodes, *Ind. Eng. Chem. Res.* 45 (2006) 3468–3473.
- [17] C.A. Martínez-Huitle, E. Brillas, Decontamination of wastewaters containing synthetic organic dyes by electrochemical methods: a general review, *Appl. Catal. B: Environ.* (2008), doi:10.1016/j.apcatb.2008.09.017.
- [18] P. Canizares, R. Paz, C. Saez, M.A. Rodrigo, Costs of the electrochemical oxidation of wastewaters: a comparison with ozonation and Fenton oxidation processes, *J. Environ. Manage.* 90 (2009) 410–420.
- [19] M. Faouzi, P. Cañizares, A. Gadri, J. Lobato, N. Bensalah, R. Paz, M.A. Rodrigo, C. Sáez, Advanced oxidation processes for the treatment of wastes polluted with azoic dyes, *Electrochim. Acta* 52 (2006) 325–331.
- [20] B. Nasr, G. Abdellatif, P. Cañizares, C. Sáez, J. Lobato, M.A. Rodrigo, Electrochemical oxidation of hydroquinone, resorcinol, and catechol on boron-doped diamond anodes, *Environ. Sci. Technol.* 39 (2005) 7234–7239.
- [21] J. Iniesta, P.A. Michaud, M. Panizza, G. Cerisola, A. Aldaz, Ch. Comninellis, Electrochemical oxidation of phenol at boron-doped diamond electrode, *Electrochim. Acta* 46 (2001) 3573–3578.
- [22] E. Brillas, M.A. Baños, M. Skoumal, P.L. Cabot, J.A. Garrido, R.M. Rodríguez, Degradation of the herbicide 2,4-DP by anodic oxidation, electro-Fenton and photoelectro-Fenton using platinum and boron-doped diamond anodes, *Chemosphere* 68 (2007) 199–209.
- [23] L. Gherardini, P.A. Michaud, M. Panizza, Ch. Comninellis, N. Vattistas, Electrochemical oxidation of 4-chlorophenol for wastewater treatment. Definition of normalized current efficiency, *J. Electrochem. Soc.* 148 (2001) 78–82.
- [24] J.S. Albuquerque, J.C. Domingos, G.L. Sant'Anna, M. Dezotti, Application of ozonation to reduce biological sludge production in an industrial wastewater treatment plant, *Water Sci. Technol.* 58 (2008) 1971–1976.
- [25] K.Y. Park, S.K. Maeng, K.G. Song, K.H. Ahn, Ozone treatment of wastewater sludge for reduction and stabilization, *J. Environ. Sci. Health Part A* 43 (2008) 1546–1550.
- [26] P. Berger, N. Karpel Vel Leitner, M. Dore, B. Legube, Ozone and hydroxyl radicals induced oxidation of glycine, *Water Res.* 33 (1999) 433–441.
- [27] F.J. Benitez, J. Beltran-Heredia, J. Torregrosa, J.L. Acero, Treatment of olive mill wastewaters by ozonation, aerobic degradation and the combination of both treatments, *J. Chem. Technol. Biotechnol.* 74 (1999) 639–646.
- [28] K.A. Segovia-Bravo, P. Garcia-Garcia, F.N. Arroyo-López, A. López-López, A. Garrido-Fernández, Ozonation process for the regeneration and recycling of Spanish green table olive fermentation brines, *Eur. Food Res. Technol.* 227 (2008) 463–472.
- [29] F.J. Beltrán, J.M. Encinar, A.A. Miguel, Nitroaromatic hydrocarbon ozonation in water. 1. Single ozonation, *Ind. Eng. Chem. Res.* 37 (1998) 25–31.
- [30] S. Dogruel, E.A. Genceli, F.G. Babuna, D. Orhon, Ozonation of non-biodegradable organics in tannery wastewater, *J. Environ. Sci. Health Part A* 39 (2004) 1705–1715.
- [31] B. Marselli, J. García-Gómez, P.A. Michaud, M.A. Rodrigo, Ch. Comninellis, Electrogeneration of hydroxyl radicals on boron-doped diamond electrodes, *Electrochem. Soc.* 150 (2003) D79.
- [32] P.A. Michaud, M. Panizza, L. Ouattara, T. Diaco, G. Foti, Ch. Comninellis, Electrochemical oxidation of water on synthetic boron-doped diamond thin film anodes, *Appl. Electrochem.* 33 (2003) 151–154.
- [33] H.D. Grimes, K.K. Perkins, W.F. Boss, Ozone degrades into hydroxyl radical under physiological conditions: a spin trapping study, *Plant Physiol.* 72 (1983) 1016–1020.
- [34] J. Staehelin, J. Hoigné, Decomposition of ozone in water: rate of initiation by hydroxide ion and hydrogen peroxide, *Environ. Sci. Technol.* 16 (1982) 676–680.
- [35] J. Hoigne, H. Bader, The role of hydroxyl radical reactions in ozonation processes in aqueous solutions, *Water Res.* 10 (1976) 377–386.
- [36] N.J. Bejarno-Perez, M.F. Suarez-Herrera, Sonophotocatalytic degradation of Congo red and methyl orange in the presence of TiO₂ as catalyst, *Ultrason. Sonochem.* 14 (2007) 589–595.
- [37] M. Khadhraoui, H. Trabelsi, M. Ksibi, S. Bouguerra, B. Elleuch, Discoloration and detoxification of a Congo red dye solution by means of ozone treatment for a possible water reuse, *J. Hazard. Mater.* 161 (2009) 974–981.
- [38] H. Ma, M. Wang, R. Yang, W. Wang, J. Zhao, Z. Shen, S. Yao, Radiation degradation of Congo Red in aqueous solution, *Chemosphere* 68 (2007) 1098–1104.
- [39] Y.M. Kolthoff, R. Belcher, *Volumetric Analysis*, vol. III, Interscience Publisher, New York, 1957.
- [40] H. Bader, J. Hoigné, Determination of ozone in water by the indigo method, *Water Res.* 15 (1981) 449–456.
- [41] A. Mokri, D. Ousse, S. Espulgas, Oxidation of aromatic compounds with UV radiation/ozone/hydrogen peroxide, *Water Sci. Technol.* 35 (1997) 95–102.
- [42] F. Al Momani, C. Sans, S. Espulgas, A comparative study of the advanced oxidation of 2,4-dichlorophenol, *J. Hazard. Mater.* 107 (2004) 123–129.
- [43] P.-A. Michaud, E. Mahé, W. Haenni, A. Perret, Ch. Comninellis, Preparation of peroxodisulfuric acid using boron-doped diamond thin-film electrodes, *Electrochem. Solid State Lett.* 3 (2000) 77.
- [44] G.D. Onstad, S. Strauch, J. Meriluoto, G.A. Codd, U.V. Gunten, Selective oxidation of key functional groups in cyanotoxins during drinking water ozonation, *Environ. Sci. Technol.* 41 (2007) 4397–4404.